Kosterlitz–Thouless transition in 1D Heisenberg antiferromagnet: An evidence based on topological properties of the ground state†

Piotr Tomczak, Piotr Jabłoński
Adam Mickiewicz University, Poznań, Poland

May 23, 2017

† This work was supported by National Science Centre Grant No. DEC-2013/08/M/ST3/00967

Outline

1. Classical phase transitions: mean field, Peierls argument, critical indices, scaling, universality, RG method

2. The Nobel Prize in Physics 2016: KT transition, Haldane conjecture, role of topology

3. Resonating valence bond states

4. Probing the Kosterlitz-Thouless transition in 1D Heisenberg antiferromagnet based on topological properties of its ground state

Classical Phase transitions

Order parameter!

System	Phase transition	Order parameter
H_2O, ^4He, Fe	liquid–solid	shear modulus
Xe, Ne, N_2, H_2O	liquid–gas	density difference
Fe, Ni	ferromagnet–paramagnet	magnetization
$RbMnF_2$, La_2CuO_4	antiferromagnet–paramagnet	staggered magnetization
^4He, ^3He	superfluid–normal liquid	superfluid density
Al, Pb, $YBa_2Cu_3O_{6.97}$	superconductor–metal	superfluid density
Li, Rb, H	Bose–Einstein condensation	condensate

$$m \propto t^{\beta}, \qquad t = \left|\frac{T_c - T}{T_c}\right|$$

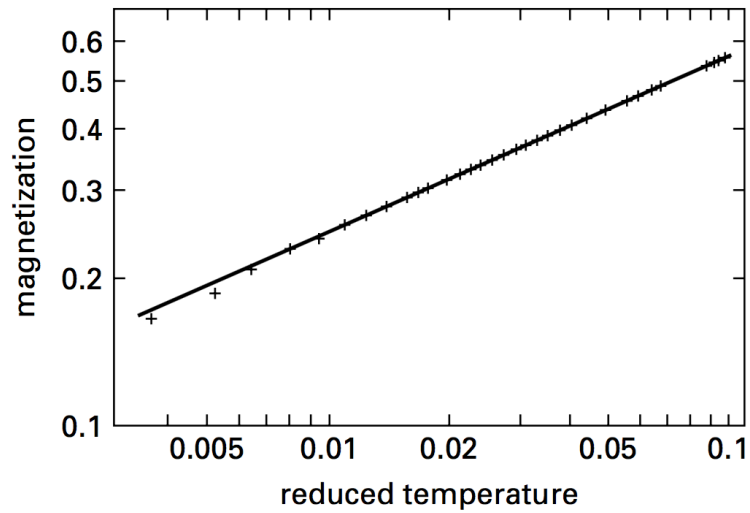

Figure 1.5 Magnetization vs. reduced temperature in nickel on a log–log plot. The slope of the straight line yields the exponent $\beta = 0.358$. (Reprinted with permission from J. D. Cohen and T. R. Carver, *Physical Review B* **15**, 5350 (1977). Copyright 1977 by the American Physical Society.)

Critical exponents

- specific heat $c(t,0) \propto t^{-\alpha}$
- order parameter $m(t,0) \propto t^{\beta}$
- susceptibility $\chi(t,0) \propto t^{-\gamma}$
- order parameter $m(h,0) \propto h^{\frac{1}{\delta}}$
- correlation length $\xi(t,0) \propto t^{-\nu}$
- correlation function $G(r,t) \propto r^{-d+2-\eta}$

K. G. Wilson and J. Kogut, The renormalization group and the ϵ expansion

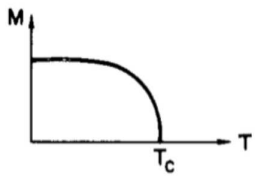

Fig. 2.1. A graph of magnetization versus temperature for a ferromagnet. T_c is the critical temperature.

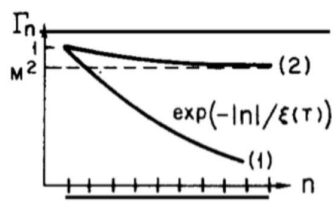

Fig. 2.2. Spin-spin correlation function versus distance between sites. Curve (1) is an example with $T > T_c$; curve (2) is an example with $T < T_c$.

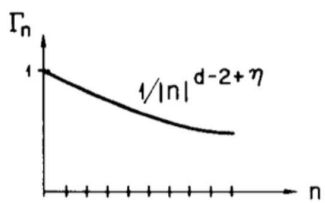

Fig. 2.3. Correlation function at the critical temperature.

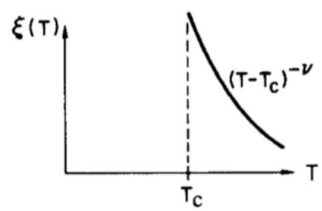

Fig. 2.4. Correlation length plotted against temperature.

Two independent critical exponents: y_T, y_H

- $\alpha = 2 - \frac{d}{y_T}$
- $\beta = \frac{d - y_H}{y_T}$
- $\gamma = \frac{2y_H - d}{y_T}$
- $\delta = \frac{2y_H}{d - y_H}$
- $\nu = \frac{1}{y_T}$
- $\eta = d + 2 - 2y_H$

Four scaling laws:

1. Rushbrooke: $\alpha + 2\beta + \gamma = 2$
2. Widom: $\gamma = \beta(\delta - 1)$
3. Fisher: $\gamma = \nu(2 - \eta)$
4. Josephson — hyperscaling: $d\nu = 2 - \alpha$

Basic Questions

- :a: Why do phase transition occur al all?
- :b: Is it possible to calculate phase diagram of a given system?
- :c: How does one calculate the values of critical exponents?
- :d: What are factors that determine which set of phenomena have the same critical exponents?
  universality:
  - dimension of space
  - dimension of order parameter
  - range of interactions

Peierls argument 1D

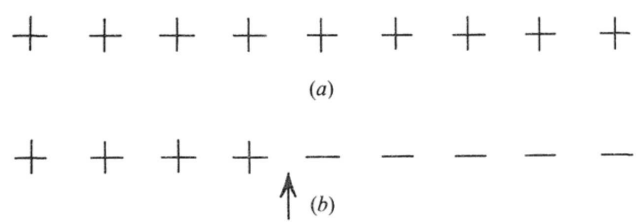

Fig. 2.11. Long-range order (*a*) in a linear chain is destroyed (*b*) by a single break.

$$\Delta F = 2J - k_B T \log L$$

Peierls argument 2D

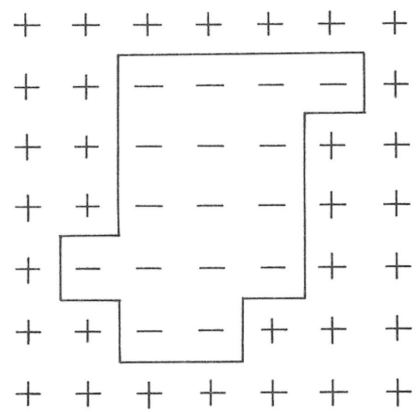

Fig. 2.12. A region of reversed Ising spins.

$$\Delta F = 2LJ - k_B T \log 3^L$$

$$\frac{k_B T_C}{J} = \frac{2}{\log 3}$$

Journal of Physics A: Mathematical and Theoretical

Exact Curie temperature for the Ising model on Archimedean and Laves lattices

Alessandro Codello

Published 20 August 2010 • 2010 IOP Publishing Ltd
Journal of Physics A: Mathematical and Theoretical, Volume 43, Number 38

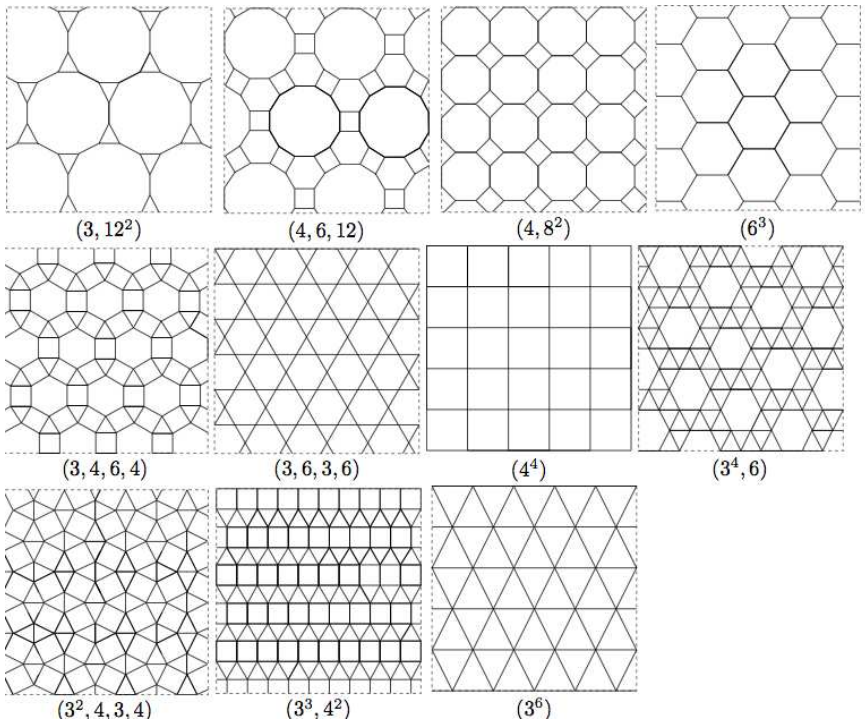

z	Λ	v_c	k_BT_c/J	$k_BT_c^*/J$
3	$(3,12^2)$	$-\frac{1}{4}-\frac{\sqrt{3}}{4}+\frac{1}{2}\sqrt{3+\frac{5\sqrt{3}}{2}}$	1.2315	5.0071
	$(4,6,12)$	$\sqrt{\frac{5+3\sqrt{3}-\sqrt{44+26\sqrt{3}}}{2}}$	1.3898	4.1363
	$(4,8^2)$	$-1-\frac{1}{\sqrt{2}}+\sqrt{\frac{5+4\sqrt{2}}{2}}$	1.4387	3.9310
	(6^3)	$\frac{1}{\sqrt{3}}$	1.5186	3.6410
4	$(3,4,6,4)$	$\frac{1}{2}-\sqrt{\frac{\sqrt{3}}{2}}+\frac{\sqrt{3}}{2}$	2.1433	2.4055
	$(3,6,3,6)$	$\frac{1}{2}-\sqrt{\frac{\sqrt{3}}{2}}+\frac{\sqrt{3}}{2}$	2.1433	2.4055
	(4^4)	$\sqrt{2}-1$	2.2692	2.2692
5	$(3^4,6)$	0.344296	2.7858	1.8757
	$(3^3,4^2)$	$\frac{1}{3}$	2.8854	1.8205
	$(3^2,4,3,4)$	0.32902	2.9263	1.7992
6	(3^6)	$2-\sqrt{3}$	3.6410	1.5186

Table 3: For each Archimedean lattice, the exact critical value of the high temperature parameter v_c, of the Curie temperature T_c and of the dual Curie temperature T_c^*, are given. The Curie temperatures T_c and T_c^* are calculated from v_c using equations (9) and (10). The values for the lattices $(4,6,12)$, $(3,4,6,4)$ and $(3^4,6)$ were not yet known exactly and agree, within errors, with the numerical values of [22, 21]. The critical values for the lattices $(3^3,4^2)$ and $(3^2,4,3,4)$ agree with the exact results of [19]. Note that the lattices $(3,4,6,4)$ and $(3,6,3,6)$ have the same critical temperature.

Theories of Phase Transitions

- Mean Field $m = \tan(zmJ + Hm)$, H - mean field (a,b)
- Landau $f(m,T) = A + Bm^2 + Cm^4 + \ldots$ (a,b)
- Scaling theory (Finite Size) (c)
- Renormalization Group $H' = R(H)$ (a,b,c,d)

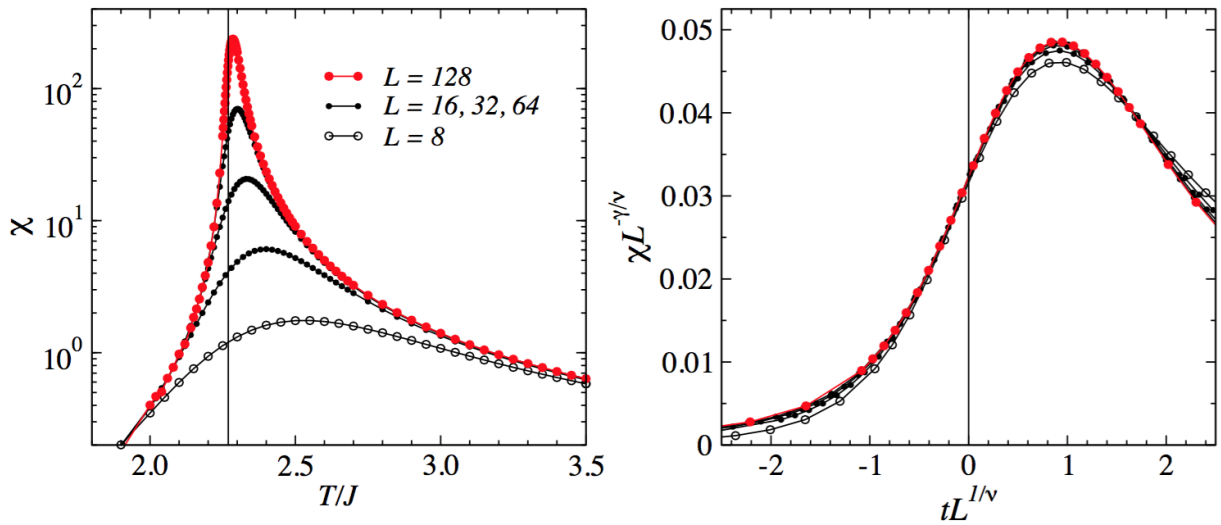

FIGURE 14. Monte Carlo results for the susceptibility (55) of the Ising model on several different $L \times L$ lattices. (a) shows the temperature dependence, with the vertical line indicating T_c. Note the vertical log scale. In (b) the data has been scaled using the exact values of the Ising exponents, $\gamma = 7/4$ and $\nu = 1$, and the exact value of T_c in $t = (T - T_c)/T_c$.

UNIVERSALITY CLASS		THEORETICAL MODEL	PHYSICAL SYSTEM	ORDER PARAMETER
$d = 2$	$n = 1$	Ising model in two dimensions	Adsorbed films	Surface density
	$n = 2$	XY model in two dimensions	Helium-4 films	Amplitude of superfluid phase
	$n = 3$	Heisenberg model in two dimensions		Magnetization
$d > 2$	$n = \infty$	"Spherical" model	None	
$d = 3$	$n = 0$	Self-avoiding random walk	Conformation of long-chain polymers	Density of chain ends
	$n = 1$	Ising model in three dimensions	Uniaxial ferromagnet	Magnetization
			Fluid near a critical point	Density difference between phases
			Mixture of liquids near consolute point	Concentration difference
			Alloy near order-disorder transition	Concentration difference
	$n = 2$	XY model in three dimensions	Planar ferromagnet	Magnetization
			Helium 4 near superfluid transition	Amplitude of superfluid phase
	$n = 3$	Heisenberg model in three dimensions	Isotropic ferromagnet	Magnetization
$d \leq 4$	$n = -2$		None	
	$n = 32$	Quantum chromodynamics	Quarks bound in protons, neutrons, etc.	

UNIVERSALITY HYPOTHESIS states that diverse physical systems behave identically near their critical points. In most cases the only factors that determine the critical properties are the dimensionality of space, d, and the dimensionality of the order parameter, n. For magnetic systems the order parameter is the magnetization, and its dimensionality is the number of components needed to describe the spin vector. Most systems with the same values of d and n are members of the same universality class and share the same critical exponents. For example, ferromagnets that resemble the three-dimensional Ising model, fluids, mixtures of liquids and certain alloys are all members of the class with $d = 3$ and $n = 1$; graphs of their properties near a critical point should all have the same form. The interpretation of some values of d and n is less obvious, and values such as $n = -2$ can be defined mathematically but correspond to no known physical system. The XY model and the Heisenberg model are similar to the Ising model but describe ferromagnets whose spin vectors have two and three components respectively.

The Nobel Prize in Physics 2016

© Trinity Hall, Cambridge University. Photo: Kiloran Howard
David J. Thouless
Prize share: 1/2

Photo: Princeton University, Comms. Office, D. Applewhite
F. Duncan M. Haldane
Prize share: 1/4

Ill: N. Elmehed. © Nobel Media 2016
J. Michael Kosterlitz
Prize share: 1/4

The Nobel Prize in Physics 2016 was divided, one half awarded to David J. Thouless, the other half jointly to F. Duncan M. Haldane and J. Michael Kosterlitz *"for theoretical discoveries of topological phase transitions and topological phases of matter"*.

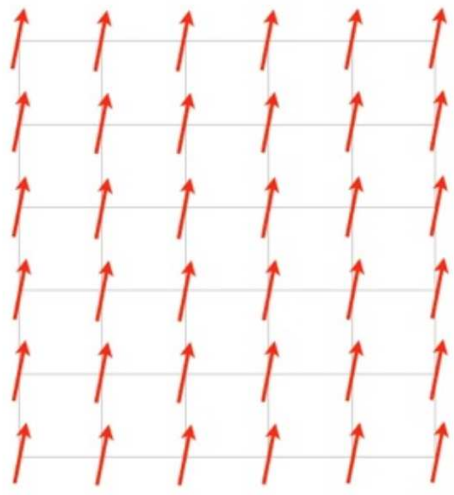

The model od XY ferromagnet

- The model: $H_{XY} = -J \sum_{nn} \mathbf{S}_i \mathbf{S}_j = -J \sum_{nn} \cos(\theta_i - \theta_j)$, ($S = \infty$, attached to squate lattice)

- continuum limit: $H_{XY} = \frac{J}{2} \int d^2 r (\nabla \theta(\vec{r}))^2$

- correlation function: $\left\langle \mathrm{e}^{i\theta(\vec{r}) - i\theta(\vec{0})} \right\rangle = \left(\frac{a}{r}\right)^{\frac{k_B T}{2\pi J}}$

- winding number: $W = \frac{1}{2\pi} \oint \nabla \theta(\vec{r}) \cdot d\vec{r}$

D.J. Thouless, *Topological Quantum Numbers in Nonrelativistic Physics*, World Scientific, 1998, page 12.

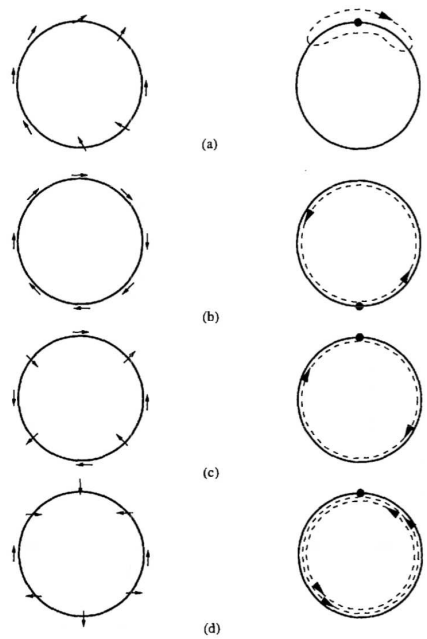

Fig. 2. Winding of a planar spin round a circle. In (a) the winding number w is zero, in (b) it is $+1$, in (c) it is -1, and in (d) it is $+2$. The direction of the spin as one goes round a loop is shown on the left of each part, while the mapping onto the order parameter space is shown on the right.

- excitations: vortices and vortex-antivortex pairs

high $T \to W = 1$ low $T \to W = 0$

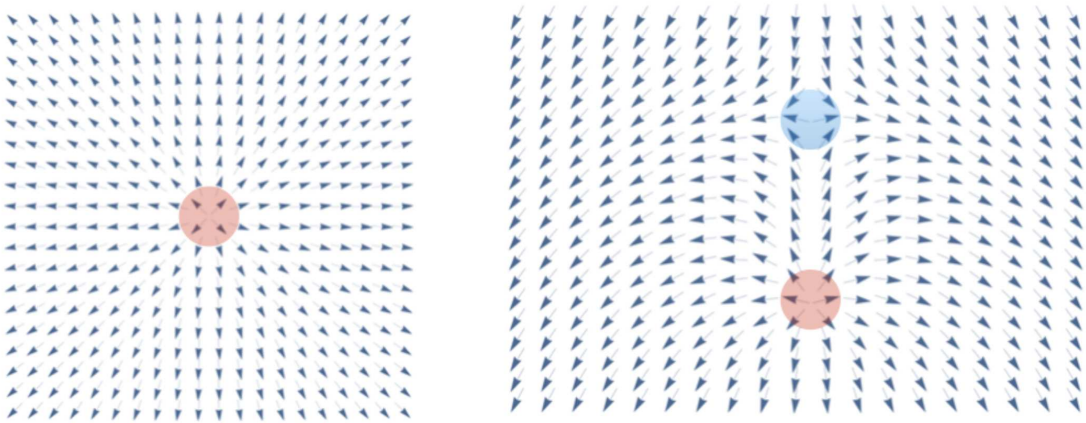

Figure 3: *To the left a single vortex configuration, and to the right a vortex-antivortex pair. The angle θ is shown as the direction of the arrows, and the cores of the vortex and antivortex are shaded in red and blue respectively. Note how the arrows rotate as you follow a contour around a vortex.*

Peierls argument

- single vortex energy: $E_v = \frac{J}{2}\int d^2r \left(\frac{1}{r}\right)^2 = J\pi \log\frac{L}{a}$
  L-system size, a-cutoff

- vortex—antivortex pair energy: $J\pi \log\frac{r}{a}$, r - v-av distance

- $F = U - TS = J\pi \log\frac{L}{a} - k_B T \log\left(\frac{L}{a}\right)^2$

- $T_{KT} = \frac{J\pi}{2k_B}$

- vortex (high T) — antivortex pair (low T) interplay

KT — correlation function

- $T < T_c$: $\left\langle \mathrm{e}^{i\theta(\vec{r})-i\theta(\vec{0})} \right\rangle = C_1$
- $T = T_c$: $\left\langle \mathrm{e}^{i\theta(\vec{r})-i\theta(\vec{0})} \right\rangle = \left(\frac{a}{r}\right)^{\frac{1}{4}}$
- $T > T_c$: $\left\langle \mathrm{e}^{i\theta(\vec{r})-i\theta(\vec{0})} \right\rangle = C_2 \mathrm{e}^{-r/\xi}$

Haldane conjecture

- $\mathcal{S}_{NLS} = \frac{S}{4}\int dxdt\ \left(\frac{1}{v}(\partial_t\vec{n})^2 - v(\partial_t\vec{n})^2\right)$
- $\mathcal{S}_{topo} = i\frac{S}{2}\int d^2x\ \vec{n}\cdot\left(\partial_1\vec{n}\times\partial_2\vec{n}\right), \qquad (x^1, x^2) = (it, x)$
- $W = i\frac{1}{4\pi}\int d^2x\ \vec{n}\cdot\left(\partial_1\vec{n}\times\partial_2\vec{n}\right)$
- $Z = \int\mathcal{D}[\vec{n}(\vec{x})]\mathrm{e}^{(-\mathcal{S}_{NLS}-\mathcal{S}_{topo})}$
- phase factor $\mathrm{e}^{-2i\pi S} \to$ spectrum gapped

Resonating Valence Bond States

P.W. Anderson suggestion (early 70's): ground states of quantum antiferromagnet is a superposition of products of singlets (valence bonds).

a. Valence bond state

b. Short range RVB,
gapfull spin liquid, long range entanglement!

c. Long range RVB,
gapless excitation

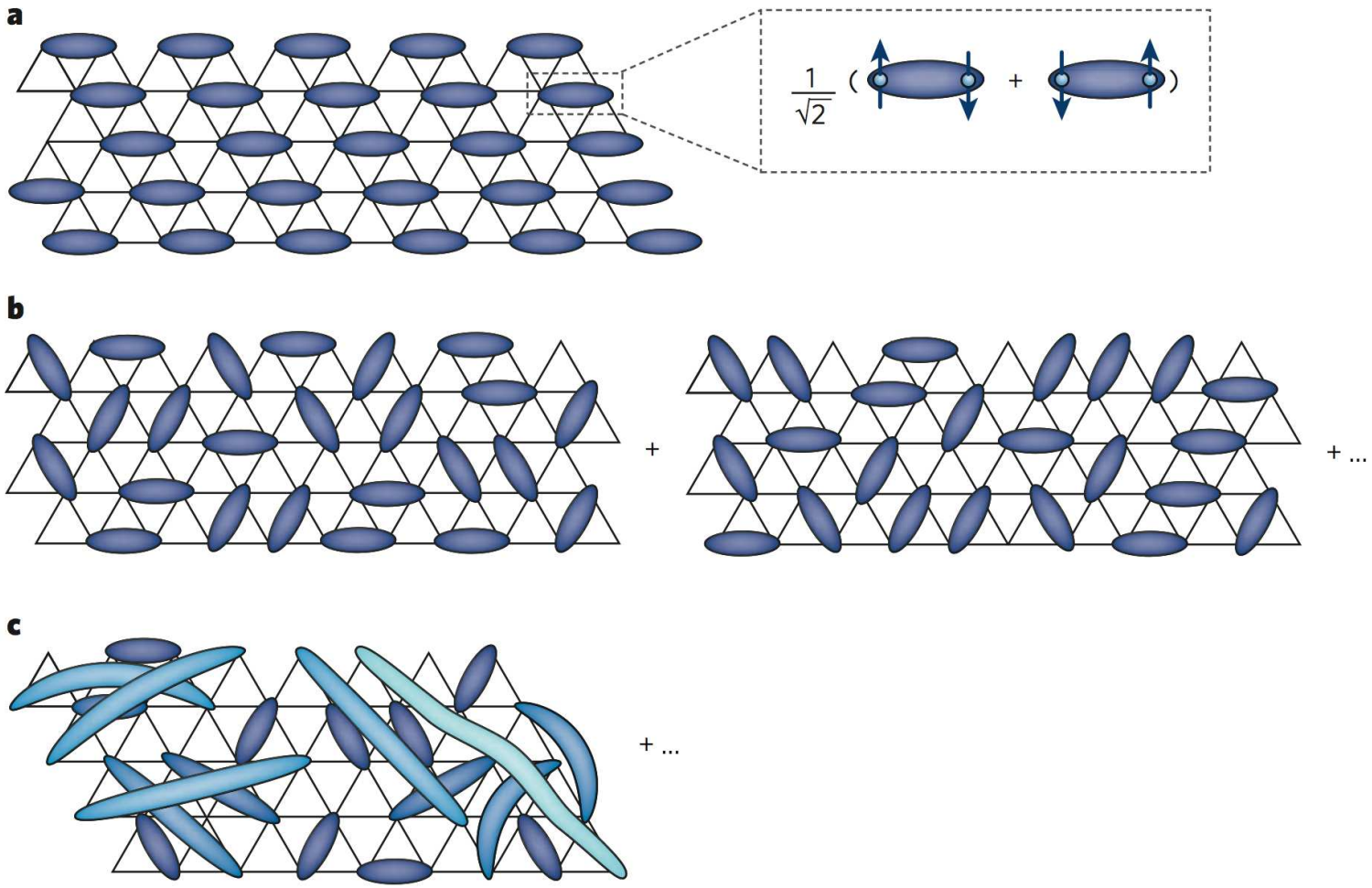
a
$\frac{1}{\sqrt{2}}$ (+)
b
+
+ ...
c
+ ...

Resonating Valence Bond States

- Non-orthogonal, over-complete set of singlet coverings
- Overlaps: $\langle\psi_1|\psi_2\rangle \sim 2^{\text{No. of loops}}$

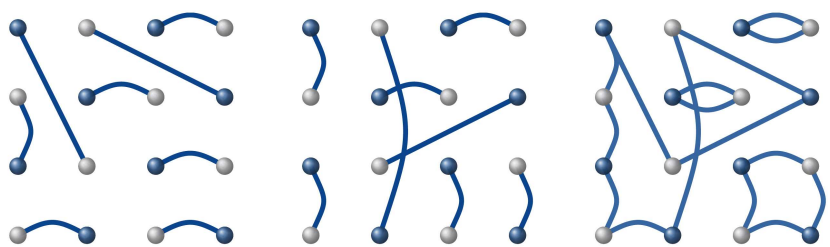

$|\psi_1\rangle$ $|\psi_2\rangle$ $\langle\psi_1|\psi_2\rangle$

The system under consideration / the metod applied

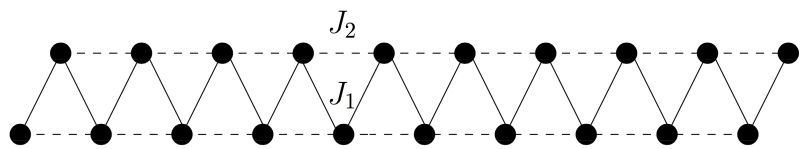

Figure 1

- $H = J_1 \sum \mathbf{S}_i \mathbf{S}_{i+1} + J_2 \sum \mathbf{S}_i \mathbf{S}_{i+2}$, $\lambda = \frac{J_2}{J_1}$.
  attached to a finite chain (up to 24 spins $\frac{1}{2}$) with PBC.

- The ground state of the above system is calculated within an exact diagonalization in RVB basis —
  generalized eigenproblem $H|\Psi\rangle = EC|\Psi\rangle$.

A very simple model

- For $\lambda < \lambda_c = 0.2411$ GS is critical with correlations $\sim \log(r)/r$ Excitations are gapless - the finite-size triplet gap $\sim 1/L$ (also with log correction).

- For $\lambda > \lambda_c$ correlations decay exponentially, triplet gap remains open in thermodynamical limit.

- The transition between these phases is known to be of Kosterlitz-Thouless type.

Computational method

- generalized eigenproblem: $H|\Psi_0\rangle = E_0 C|\Psi_0\rangle$
  C - the matrix of scalar products $\langle c_k|c_l\rangle$

- Basis dimension:
  16 spins - 1430×1430
  18 spins - 4862×4862
  20 spins - 16786×16786
  22 spins - 58786×58786
  24 spins - 280212×280212

- numerical differentiation
  $$\frac{d}{d\lambda}\psi = \Big(3(\psi_{i-4} - \psi_{i+4}) + 32(-\psi_{i-3} + \psi_{i+3}) + 168(\psi_{i-2} - \psi_{i+2}) + 672(-\psi_{i-1} + \psi_{i+1})\Big)/840$$

RVB basis and winding numbers

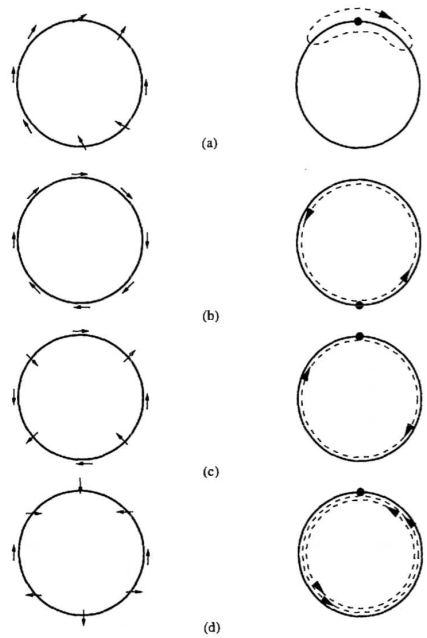

Fig. 2. Winding of a planar spin round a circle. In (a) the winding number w is zero, in (b) it is $+1$, in (c) it is -1, and in (d) it is $+2$. The direction of the spin as one goes round a loop is shown on the left of each part, while the mapping onto the order parameter space is shown on the right.

D.J. Thouless, *Topological Quantum Numbers in Nonrelativistic Physics*, World Scientific, 1998, page 12.

RVB basis and winding numbers

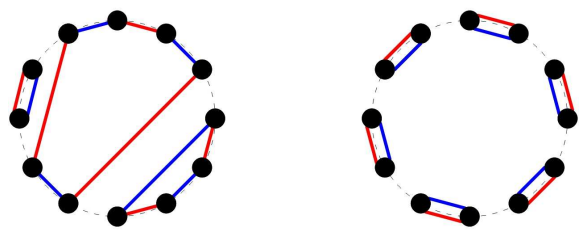

Figure 2: Examples of representing scalar products $\langle c_k | c_l \rangle$ of two basis functions $\langle c_k |$ (red) and $| c_l \rangle$ (blue) in a 12-spin system. The "transition graph" on the left is non contractible (contains 3 loops, its winding number equals to 1, topological sector W1), whereas on the right is contractible (contains 6 loops, its winding number equals to 0, topological sector W0).

$$|\Psi_0\rangle = \sum_i \alpha_i(\lambda)|c_i\rangle, \quad \langle\Psi_0|\Psi_0\rangle = \sum_{i,j} \alpha_i\alpha_j\, 2^{\mathcal{N}(c_i,c_j)}$$

where $\langle c_k|c_l\rangle = 2^{\mathcal{N}(c_k,c_l)}$ with $\mathcal{N}(c_k, c_l)$ being a number of loops arising when the coverings $\langle c_k|$ and $|c_l\rangle$ are drawn simultaneously on the same lattice.

- α_i are real!
- $\langle\Psi_0|\Psi_0\rangle = \sum_{i,j} \alpha_i\alpha_j\, 2^{\mathcal{N}(c_i,c_j)}\Big|_{W0} + \sum_{i,j} \alpha_i\alpha_j\, 2^{\mathcal{N}(c_i,c_j)}\Big|_{W1}$.
- $\langle\partial_\lambda\Psi_0|\Psi_0\rangle = -\langle\Psi_0|\partial_\lambda\Psi_0\rangle = 0$ (from normalization)
- $\langle\Psi_0|\partial_\lambda\Psi_0\rangle = \sum_{i,j} \alpha_i\partial\alpha_j\, 2^{\mathcal{N}(c_i,c_j)}\Big|_{W0} + \sum_{i,j} \alpha_i\partial\alpha_j\, 2^{\mathcal{N}(c_i,c_j)}\Big|_{W1}$.

The scalar product and its derivatives in topological sectors

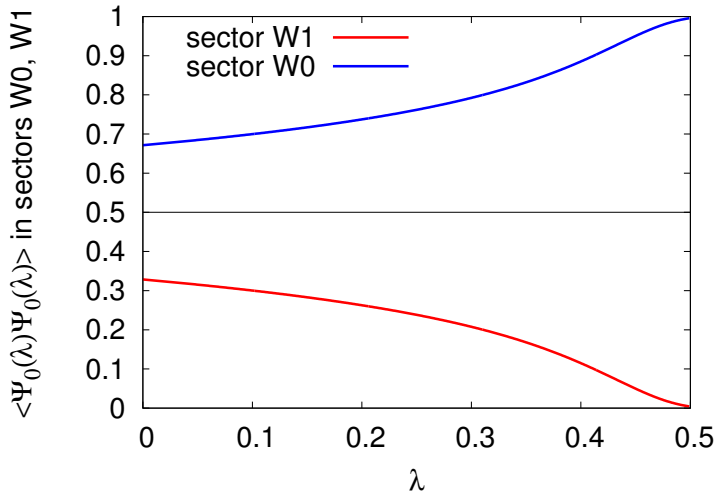

Scalar product $\langle\Psi_0(\lambda)|\Psi_0(\lambda)\rangle$ in 24-spin system split between topological sectors W0 and W1.

$$E_0(\lambda) = E_0^{W0}(\lambda) + E_0^{W1}(\lambda)$$

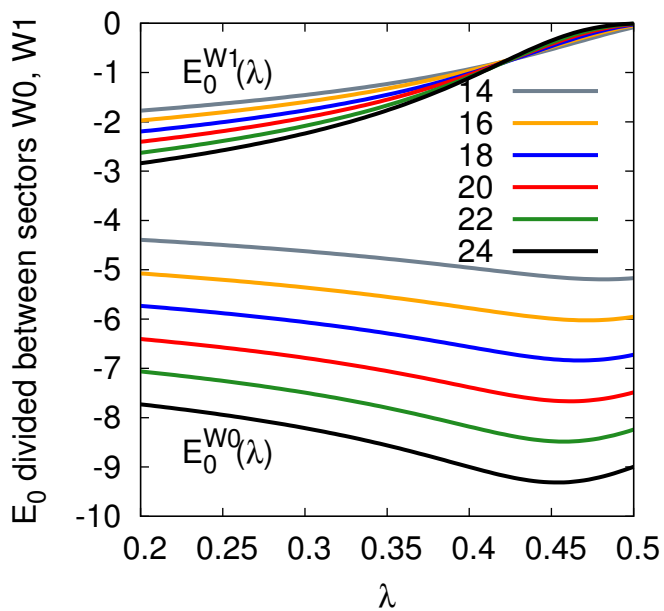

The ground state energy $E_0(\lambda)$ divided into sectors W0 and W1 in systems up to 24 spins .

Energy-entropy (Peierls) argument

- the interplay between contractible and noncontractible objects leads to a phase transition

- The energy of a non contractible loop is of the order $-\frac{3}{4}L(1-\lambda)$
  Two contractible coverings have an energy $-\frac{3}{4}\frac{L}{3}(1-\lambda)$.
  The difference $\frac{L}{2}(1-\lambda)$, increases linearly with L.

- The creation of a non contractible cowering may be done in $\frac{1}{2}C^2_{L/2}$ ways ($C_{L/2} = \frac{L!}{(L/2)!(L/2+1)!}$).

- $\frac{L}{2}(1-\lambda_c) - \lambda_c \mathrm{log}(\frac{1}{2}C^2_{L/2}) = 0$

- eventually, for large L, $\lambda_c = \frac{1}{1+4\log 2} \approx 0.265$ (which should be compared with 0.241).

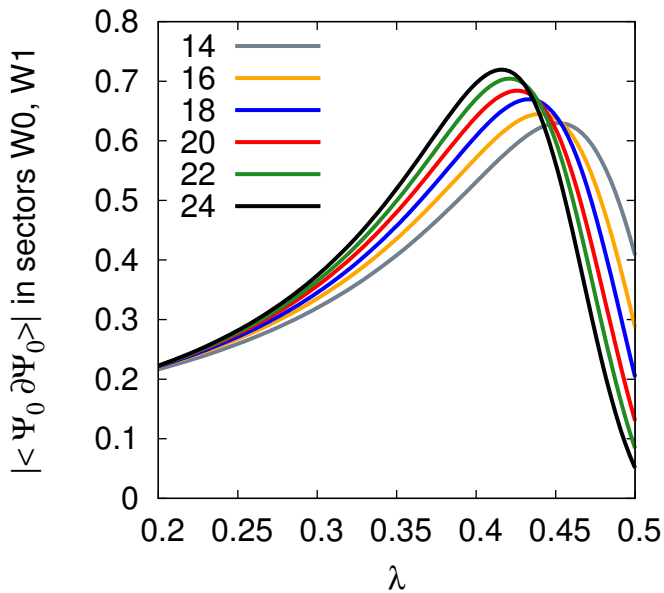

The absolute value of the scalar product derivative $|\langle\Psi_0|\partial\Psi_0\rangle|$ with respect to λ in sectors W0 and W1.

$$\chi_f(\lambda) = \frac{1}{L}\langle \partial_\lambda \Psi_0 | \partial_\lambda \Psi_0 \rangle = \chi_f^{W0}(\lambda) + \chi_f^{W1}(\lambda)$$

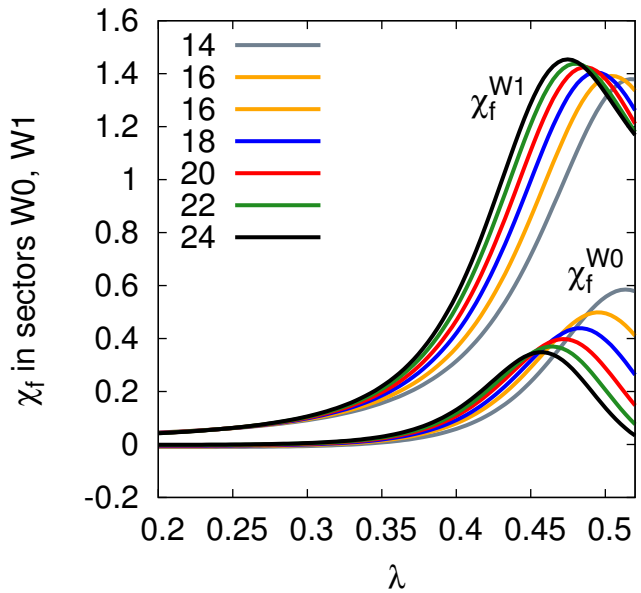

The fidelity susceptibility per spin, $\frac{1}{L}\langle \partial\Psi_0 | \partial\Psi_0 \rangle$ in systems up to L=24 spins as a function of the parameter $\lambda = J_2/J_1$.

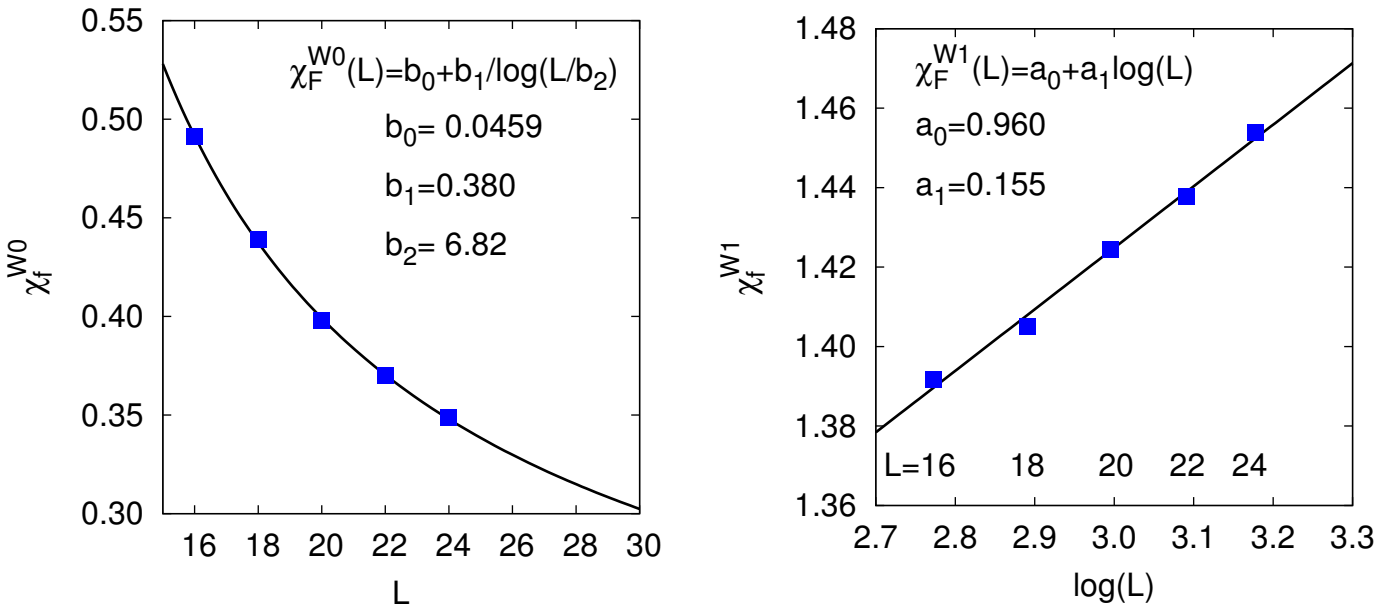

The fidelity susceptibility peak heights as a function of L in the W0 sector (left) and as a function of $\log(L)$ in the W1 sector (right).

- for $L \to \infty$ $\chi_f(\lambda)$ is logarithmically divergent

- this differs from the results [Phys.Rev. B 91, 014418 (2015)], obtained for 1D XXZ Heisenberg spin-$\frac{1}{2}$ system with open boundary conditions (OBC), pointing that fidelity susceptibility is finite

- if we would have examine the scaling of χ_f with respect to L without its splitting into topological sectors, we would have received also the finite value of χ_f for $L \to \infty$ with logarithmic correction

- while examining topological phase transitions it is better to use periodic boundary conditions

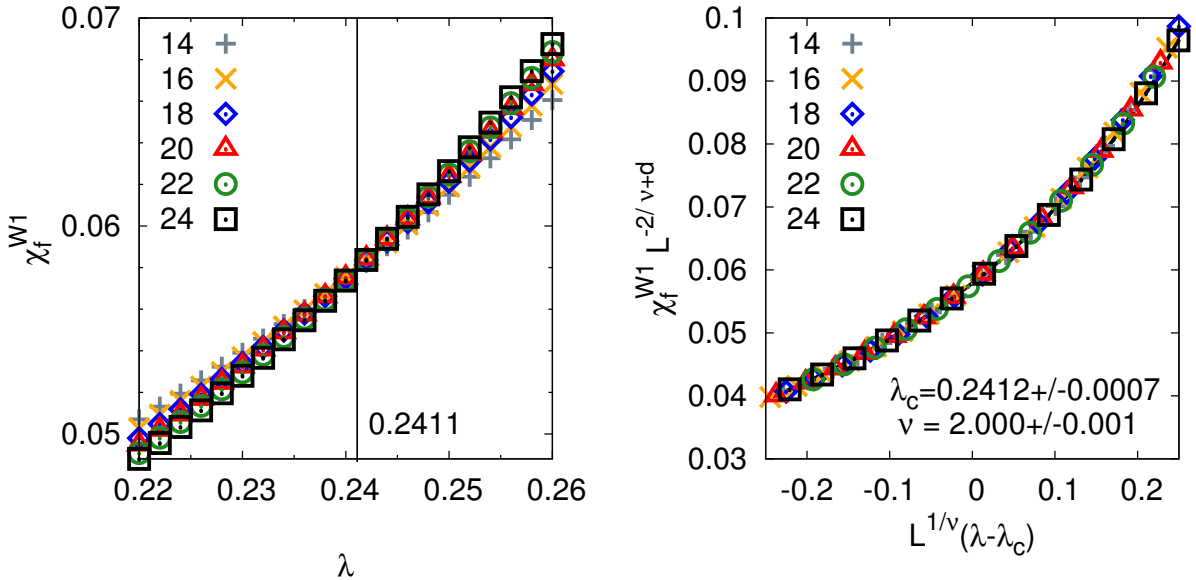

The scaling collapse of the fidelity susceptibility from sector W1 for systems with L =16-24 spins. The optimal values of $\lambda_c = 0.2412$ and exponent $\nu = 2.000$ are found. The errors were estimated by finding the collapse several times taking the numerical data with Gaussian noise with standard deviation equal to the accuracy of numerical diferentiation.

Relation to geometric phase

- if $\langle\Psi_0|\Psi_0\rangle| \propto$ geometric phase,
- then $\frac{\partial}{\partial\lambda}|\langle\Psi_0|\Psi_0\rangle| \sim a_0 + a_1 \log L$ at QPT

Shi-Liang Zhu, *Scaling of Geometric Phases Close to the Quantum Phase Transition in the XY Spin Chain*, Phys. Rev. Lett. 96, 077206 (2006).

Angelo C.M. Carollo and Jiannis K. Pachos, *Geometric Phases and Criticality in Spin-Chain Systems*, Phys. Rev. Lett. 95, 157203 (2005).

Geometric phase: rotate spins on odd and even positions around the z direction by angles ϕ and $-\phi$, respectively. This defines a new, ϕ-dependent basis in which the spectrum of the Hamiltionan remains unaltered. Under this transformation each singlet entering to a given basis function transformes as follows $|s\rangle = \frac{1}{\sqrt{2}}(|\uparrow\downarrow\rangle - |\downarrow\uparrow\rangle) \rightarrow |s'\rangle = \frac{1}{\sqrt{2}}(\mathrm{e}^{i\frac{\phi}{2}}|\uparrow\downarrow\rangle - \mathrm{e}^{-i\frac{\phi}{2}}|\downarrow\uparrow\rangle)$,

$\int \langle s'|\frac{\partial s'}{\partial \phi}\rangle d\phi$, for two spins-$\frac{1}{2}$ coupeld antiferromagnetically in their ground state, due to equal contributions (with opposite sign) from the term $(\mathrm{e}^{i\frac{\phi}{2}}|\uparrow\downarrow\rangle$ and the term $\mathrm{e}^{-i\frac{\phi}{2}}|\downarrow\uparrow\rangle)$ equals to 0. The same is true for any finite system, but one can overcome this difficulty, by acumulating the geometric phase for only one term and similarly for larger systems.

The geometric phase, $\beta_g/\mathcal{N}_s$ for the groundstate $|\Psi_0(\phi)\rangle$, accumulated by varying the angle ϕ from 0 to π is proportional to the $-i\pi\langle\Psi_0|\Psi_0\rangle$ and seems to be not λ-dependent one.

The absolute value of its derivative in sectors W0 and W1 displays a well-marked peak at $\lambda^*(L) > \lambda_c$, which shifts towards λ_c with increasing L. The value of $\frac{d\beta_g}{d\lambda}$ diverges $\frac{\partial}{\partial\lambda}\beta_g/\mathcal{N}_s \sim a_0 + a_1 \log L$ with a_1=2.272.

It is possible to extract a critical exponent ν from the scaling of the function $B = (1 - \mathrm{e}^{\frac{d\beta_g(\lambda(L))}{d\lambda} - \frac{d\beta_g(\lambda^*(L))}{d\lambda}}) \propto L^{1/\nu}(\lambda(L) - \lambda^*(L))$

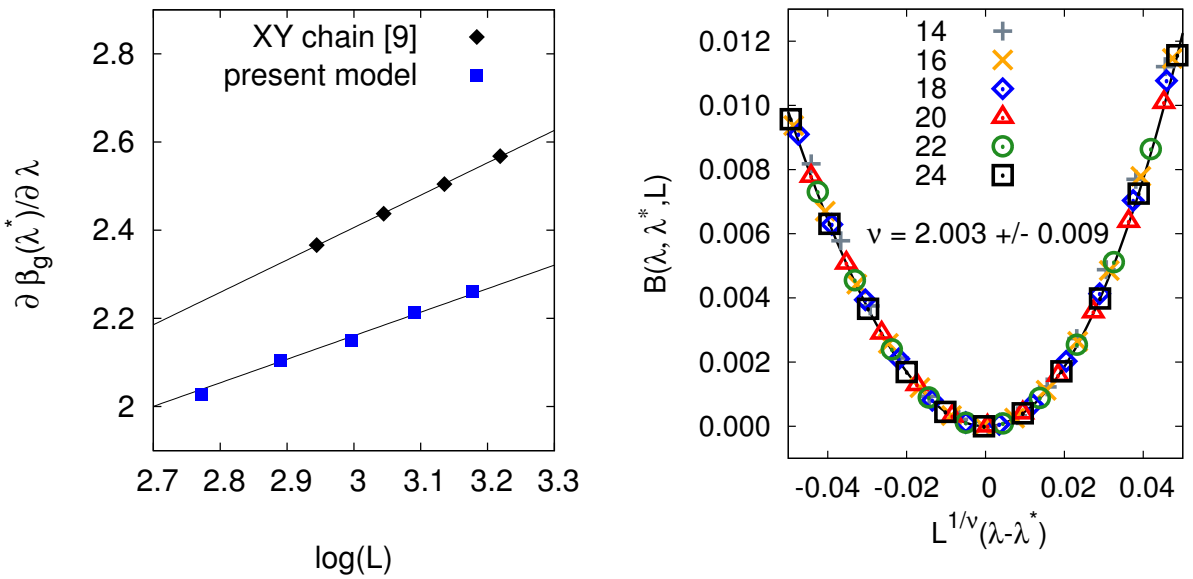

The value of the function $B(\lambda, \lambda^*, L)$ versus $L^{1/\nu}(\lambda - \lambda^*)$ for system sizes L =16-24. As expected from the finite size scaling ansatz the data for different system sizes collapse on a single curve for $\nu = 2.003$. The error is estimated as explained in the caption of previous Figure.

Summary

- Finite size scaling of $\langle \partial\Psi_0 | \partial\Psi_0 \rangle_{W1}$ enables to locate quantum critical point $\lambda_c = 0.2411$ and to find critical exponent $\nu = 2$ in a frustrated spin system with Kosterlitz-Thouless phase transition.

- The term $\langle \Psi_0 | \partial\Psi_0 \rangle \Big|_{W0,W1}$ is related to geometric phase. Finite size scaling of the geometric phase is the independent test for $\lambda_c = 0.2411$ and $\nu = 2$.

- We hope that the presented result open the way for further exploration of critical phenomena in systems in which there is no possibility to identify an order parameter.